*32nd EPS Conference on Plasma Phys. Tarragona, 27 June - 1 July 2005 ECA Vol.**29C**, P-2.017 (2005)*

Impact of Magnetic Configuration on Edge Radial Electric Field: MAST-ASDEX Upgrade Simulation with B2SOLPS5.0

V. Rozhansky[1], E. Kaveeva[1], S. Voskoboynikov[1], G. Counsell[2], A. Kirk[2], H. Meyer[2], D. Coster[3], G. Conway[3], J. Schirmer[3], R. Schneider[4] and ASDEX Upgrade Team

[1]*St.Petersburg State Polytechnical University, Polytechnicheskaya 29, 195251 St.Petersburg, Russia*
[2]*EURATOM/UKAEA Fusion Association, Culham Science Centre, Abingdon, Oxon, OX14 3DB, UK*
[3]*Max-Planck Institut für Plasmaphysik, EURATOM Association, D-85748 Garching, Germany*
[4]*Max-Planck Institut für Plasmaphysik, EURATOM Association, D-17491 Greifswald, Germany*

Introduction

Detailed modeling of the radial electric field in the separatrix vicinity has been performed for three divertor configurations: Upper Double Null (UDND), Lower Double Null (LDND) and Connected Double Null (CDN) with the B2SOLPS5.0 transport code. The aim of the work was to understand the results of the observations on MAST and ASDEX Upgrade (AUG), where easier access to the H-mode was obtained for the CDN case. Radial electric field and toroidal rotation profiles were compared for all three configurations both for low field side (LFS) and high field side (HFS) cases.

Simulation results

For MAST three Ohmic shots №7656 (LDND), №7666 (CDN) and №7669 (UDND) with similar radial profiles of temperature and density in the core but different geometry of the separatrices were simulated. For AUG shot №19415 with equilibrium changing in time from LDND through CDN to UDND configuration was simulated. The following modeling parameters were chosen: i) MAST: plasma density at the inner boundary (6.3 *cm* inside the inner separatrix at the outer midplane) $n_e\big|_{core} = 2 \cdot 10^{19} m^{-3}$, electron and ion temperatures $T_e\big|_{core} = 100 eV$, $T_i\big|_{core} = 100 eV$, turbulent diffusion coefficient $D = 1\ m^2/s$, electron and ion heat conductivity $\chi_e = 2.5\ m^2/s$, $\chi_i = 1.5\ m^2/s$, ii) AUG: plasma density at the inner boundary (7 *cm* inside the inner separatrix at the outer midplane) $n_e\big|_{core} = 2.85 \cdot 10^{19} m^{-3}$, $T_e\big|_{core} = 275 eV$, $T_i\big|_{core} = 275 eV$, $D = 0.5\ m^2/s$, $\chi_{e,i} = 0.7 m^2/s$. The MAST radial electric fields in the simulations for the three configurations at the LFS midplane are shown in Fig.1. The simulations for AUG are shown in Fig. 2. For MAST the LFS radial electric fields just inside the separatrix in CDN and UDND cases are negative and comparable, while in the

LDND case the electric field is smaller in absolute value. For AUG the CDN and LDND electric fields are comparable while the UDND electric field is significantly smaller in absolute value. Experimental results for AUG are presented in Fig. 3. Measurements were performed using Doppler reflectometry diagnostics [1]. As can be seen for AUG, the tendency obtained in the simulations is similar to that observed in the experiment: the UDND field is smaller in absolute value than for the two other cases.

The calculated radial electric field profiles at the HFS midplane are shown in Figs. 4-5. One can see strong spikes in the CDN radial electric field profiles at the separatrix both for AUG and MAST shots. These spikes disappear in the LDND and UDND configurations. The parallel velocity at the LFS midplane is shown in Fig. 6 for three MAST shots. In the CDN case the parallel velocity is a few km/s more positive (negative sign corresponds to the co-current direction) at the core boundary. This is consistent with observation [2]. The strong counter-current parallel velocity at the HFS in the CDN case, Fig. 7, corresponds to the counter-current Pfirsch-Schlueter flux observed on C-mod [3]. The dependence of the LFS radial electric field on the divertor configuration might be explained by the change of parallel fluxes in the SOL. The parallel fluxes are transported through the separatrix by turbulent viscosity and generate an additional electric field. However, it is difficult to explain the observed easier access to the H-mode in the CDN configurations by the change of LFS electric field.

The origin of the spike of the radial electric field at the HFS for the CDN case is connected with the different potential drops between the divertor plates and the equatorial midplane in the LFS and HFS SOL, which are isolated in the CDN case. Indeed, these potential drops are determined by the parallel momentum balance equation for electrons, i.e. by the density and electron temperature profiles. These profiles are different in the disconnected LFS and HFS SOL. On the other hand, the separatrix should be almost at the same potential due to the high conductivity on the closed field lines. The separatrix potential is determined by the larger LFS SOL. Therefore, the potential drop should exist in the separatrix vicinity at HFS. This spike might cause the turbulence suppression everywhere both for HFS and LFS and thus might decrease the L-H transition threshold in the CDN case.

Discussion

The impact of geometrical factors on the radial electric field structure at the LFS midplane is connected with the change of the parallel fluxes in the scrape-off layer, which are

transported through the separatrix due to turbulent viscosity and diffusivity. These parallel fluxes in the core region are not divergent free and hence change the particle balance. To keep the divergence of all the fluxes equal to the source term an additional radial electric field arises, which produces the necessary additional poloidal $\vec{E} \times \vec{B}$ drift. Simulations demonstrate, however, that the difference in radial electric fields for different configurations at the LFS equatorial midplane is not so pronounced. Thus the alternative possible mechanism for lowering the L-H transition threshold for the CDN case might be the turbulence suppression by the shear of the electric field inside the spike formed at the HFS equatorial midplane. The spike is observed in all MAST and AUG runs including special test runs. The amplitude of the spike depends on the difference in potential drops between the divertor plates and the equatorial midplanes in the HFS and LFS SOL. The amplitude of the spike might be controlled by the change of LFS or HFS SOL parameters. For example, the change of parallel ion heat conductivity in the test run reduces the spike amplitude in AUG by a factor of two. Another possible explanation for the lower L-H transition threshold in the CDN case might be a lower level of turbulence when the two X-points are located at the same separatrix.

Acknowledgements This work was funded partly by the United Kingdom Engineering and Physical Sciences Research Council and by EURATOM.

References

1. G D Conway et al PPCF **46** (2204) 951.
2. H Meyer et al, PPCF **47** (2005) 843.
3. B LaBombard et al, Nuclear Fusion **44** (2004) 1047.

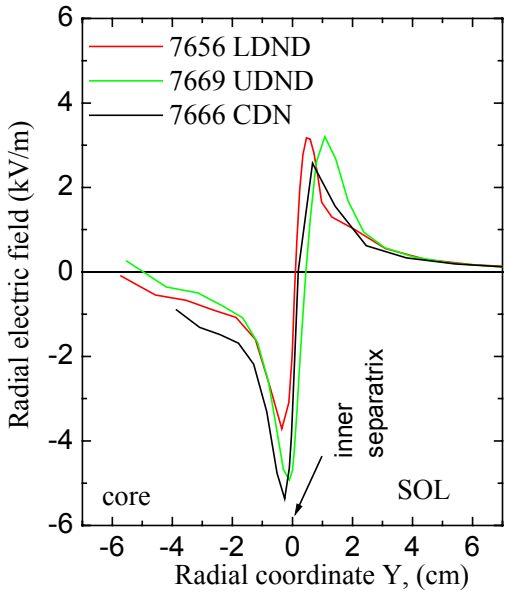

Fig. 1. Calculated radial electric fields at the LFS midplane for different MAST configurations, shots №7656, 7666, 7669.

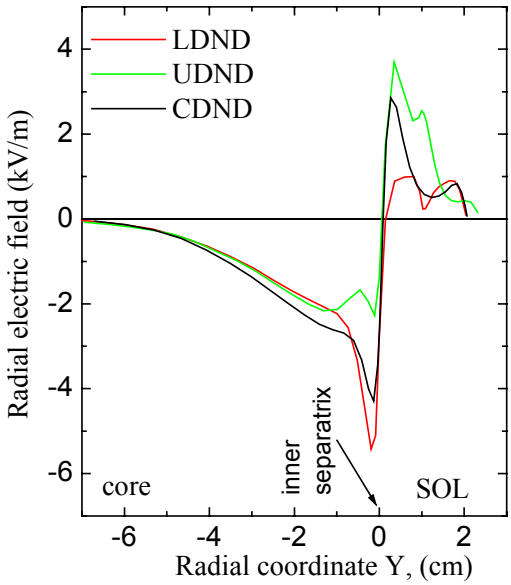

Fig. 2. Calculated radial electric fields at the LFS midplane for different AUG configurations in the shot №19415

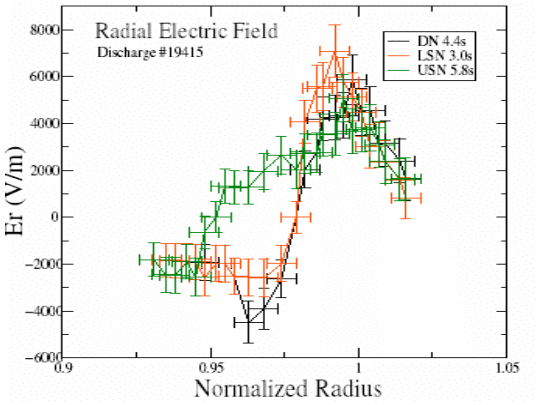

Fig. 3. Experimental radial electric field profiles at the LFS midplane for different AUG configurations in the shot №19415.

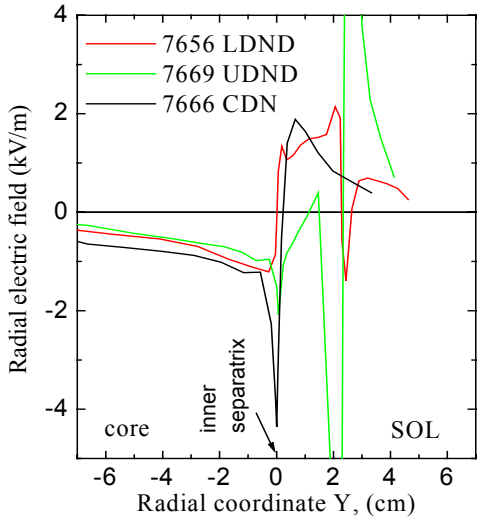

Fig. 4. Calculated radial electric fields at the HFS midplane for different MAST configurations, shots №7656, 7666, 7669.

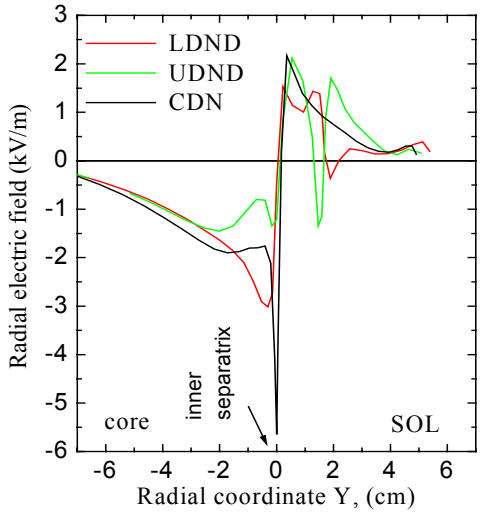

Fig. 5. Calculated radial electric fields at the HFS midplane for different AUG configurations in shot №19415

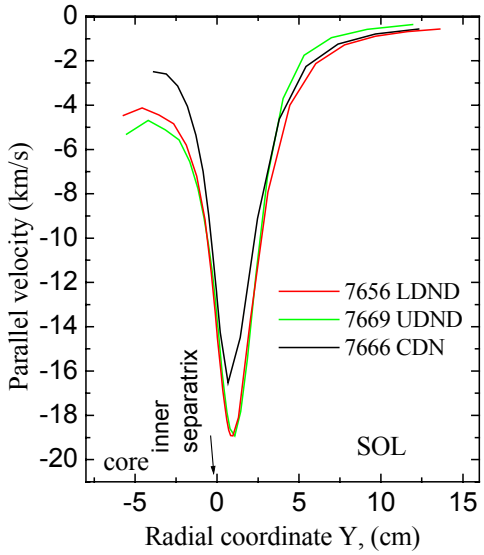

Fig. 6. Calculated parallel velocity profiles at the LFS midplane for different MAST configurations, shots №7656, 7666, 7669.

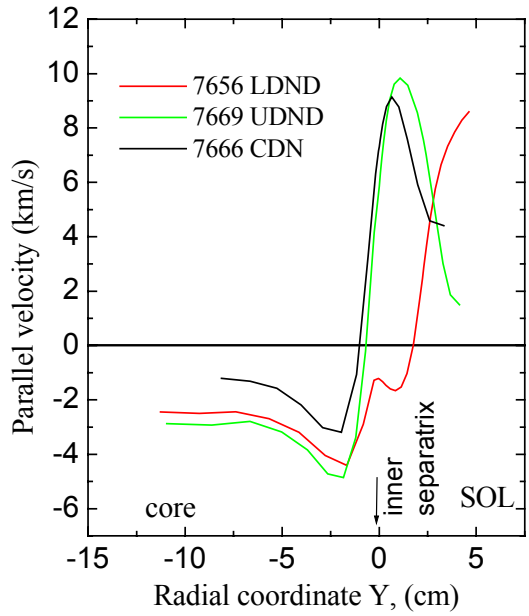

Fig. 7. Calculated parallel velocity profiles at the HFS midplane for different MAST configurations, shots №7656, 7666, 7669